Polymer Chemistry

Carborane RAFT Agents as Tunable and Functional Molecular Probes for Polymer Materials

Journal:	*Polymer Chemistry*
Manuscript ID	PY-ART-02-2019-000199
Article Type:	Paper
Date Submitted by the Author:	07-Feb-2019
Complete List of Authors:	Spokoyny, Alex; UCLA, Chemistry and Biochemistry Messina, Marco; University of California, Los Angeles, Chemistry and Biochemistry Graefe, Christian; University of Minnesota System, Department of Chemistry Chong, Paul; UCLA, Chemistry and Biochemistry Ebrahim, Omar; UCLA, Chemistry and Biochemistry Pathuri, Ramya; UCLA, Chemistry and Biochemistry Bernier, Nicholas; UCLA, Chemistry and Biochemistry Mills, Harrison; UCLA, Chemistry and Biochemistry Rheingold, Arnold; University of California, Department of Chemistry and Biochemistry Frontiera, Renee; University of Minnesota, Chemistry Maynard, Heather; University of California, Los Angeles, Chemistry and Biochemistry

Journal Name

ARTICLE

Carborane RAFT Agents as Tunable and Functional Molecular Probes for Polymer Materials

Received 00th January 20xx,
Accepted 00th January 20xx

DOI: 10.1039/x0xx00000x

www.rsc.org/

Marco S. Messina,*[a] Christian T. Graefe,[c] Paul Chong,[a,e] Omar M. Ebrahim,[a] Ramya S. Pathuri,[a] Nicholas A. Bernier,[a] Harrison A. Mills,[a] Arnold L. Rheingold,[d] Renee R. Frontiera,*[c] Heather D. Maynard,*[a,b] and Alexander M. Spokoyny*[a,b]

Functional handles appended to polymer chain ends are important tools often used as spectroscopic probes for determining polymer structure, affinity labels, and as reactive handles for the conjugation of functional payloads. An easily tunable molecular handle able to carry out multiple functions simultaneously would be of significant use at the polymer, materials, and biology interface. Here, we report the development of carborane-containing chain transfer agents (CTAs, commonly referred to as RAFT agents) which are used in reversible addition-fragmentation chain transfer (RAFT) polymerization. These carborane RAFT agents establish control over polymerization processes leading to monodisperse (*Đ* = 1.03-1.15) polymers made from *N*-isopropylacrylamide, styrene, 4-chlorostyrene, and methyl acrylate monomers. The tunable nature of the carborane-based scaffold appended on the polymer chain end serves as a general ^{1}H NMR spectroscopic handle, which can be used to elucidate polymer molecular weight *via* end-group analysis. Isothermal titration calorimetry (ITC) measurements show that synthesized carborane terminated polymers exhibit strong binding to β-cyclodextrin with an affinity (Ka) of 9.37x104 M^{-1}, thereby demonstrating its potential use as an affinity label. Additionally, we show that the free B-H vertices on the carborane RAFT agents exhibit a Raman vibrational signal at ~2549 cm^{-1}, a Raman-silent region for biological milieu, indicating its potential utility as an innate Raman active probe. The reported carborane RAFT agents bolster the expanding toolbox of molecular probes and serve as tunable platforms for incorporating additional and complementary handles for tailoring chain-end functionality and facilitating polymer analysis.

Introduction

There exist myriad molecular tools employed at the interface of polymer chemistry and biology to help elucidate the structure and/or functions of molecules. These tools come in the form of small molecule probes, affinity labels, and spectroscopic handles frequently applied to polymer chain ends.[1-10] Conjugation of such tools to polymer end groups is typically performed through rational design of polymer initiators or chain transfer agents, which are retained on the ends of polymers made from controlled polymerization processes.[11-19] Specifically, RAFT polymerization is a versatile method used to obtain polymers of uniform molecular weight.[20-23] This method has gained widespread attention due to its broad monomer scope, solvent compatibility, and ease of constructing well-defined macromolecular architectures, such as block co-polymers and brush polymers.[22, 24] Key to this method is the use of the RAFT agent (Figure 1).[25-28]

Figure 1. (A) Structures of frequently utilized chain transfer agents in RAFT polymerization. (B) Introduction of carborane RAFT agents as multi-purpose functional molecular probes and affinity label.

[a] *Department of Chemistry and Biochemistry, University of California, Los Angeles, 607 Charles E. Young Drive East, Los Angeles, California 90095-1569, United States. Email: messina@chem.ucla.edu; maynard@chem.ucla.edu; spokoyny@chem.ucla.edu*
[b] *California NanoSystems Institute, University of California, Los Angeles, 570 Westwood Plaza, Los Angeles, California 90095-1569, United States.*
[c] *Department of Chemistry, University of Minnesota, Minneapolis, Minnesota, 55455, United States. Email: rrf@umn.edu*
[d] *Department of Chemistry and Biochemistry, University of California, San Diego, 9500 Gilman Drive, La Jolla, California, 92093, United States.*
[e] *Department of Chemistry, Stanford University, 333 Campus Dr., Stanford, California, 94305, United States.*
†Electronic Supplementary Information (ESI) available: Supplemental Information includes experimental procedures and characterization of small molecules and polymers. CCDC: 1879544. See DOI: 10.1039/x0xx00000x

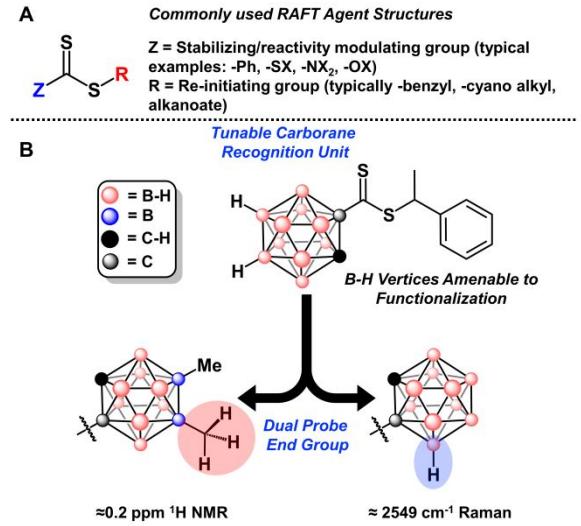

The RAFT agent confers control over polymerization processes through a reversible radical chain transfer reaction to and from the thiocarbonyl moiety. By greatly reducing the amount of active radicals capable of polymerization, thereby decreasing unwanted termination pathways, polymers with narrow molecular weight distributions are formed.[26, 27] RAFT agents are comprised of thiocarbonylthio compounds, common classes of which include dithioesters, xanthates, trithiocarbonates, and dithiocarbamates (Figure 1A).[26, 27, 29] The RAFT agent structure can be conceptually split into two parts wherein the "Z" group modulates the rates of addition and fragmentation during reversible chain transfer on the thiocarbonyl carbon and determines the stability of the intermediate radical, and the "R" group functions to re-initiate polymerization of another monomer upon homolytic cleavage from the RAFT agent structure (Figure 1A).[26, 30] Both the R and Z groups are incorporated on the polymer chain end upon termination. As a result, the structure of the RAFT agent is often tailored to serve as a functional handle and/or probe for characterization.[2, 5, 31, 32] Some examples of functional handles include the use of carboxylic acid, succimidyl ester, azide, maleimide, aminooxy, or pyridyl disulfide functionalized RAFT agents, which serve as conjugation sites for molecular cargo such as fluorescence tags, affinity labels, and biomolecules.[2, 7, 14, 15, 33-42] Trimethylsilyl (TMS) substituted RAFT agents have also served as spectroscopic handles in the determination of polymer molecular weight *via* ^{1}H NMR spectroscopy.[5]

While these functional RAFT agents are able to perform one or two tasks, tunable and stable RAFT agents capable of performing multiple tasks simultaneously while retaining modularity are rare. We envisaged *ortho*-carborane functionalized RAFT agents as being ideally suited to interface many different applications through their ability to act as spectroscopic probes, easily modifiable molecular conjugation sites, and as affinity labels. Icosahedral carboranes ($C_2B_{10}H_{12}$) are boron-rich molecules which exhibit 3-dimensional (3D) electron delocalization non-uniformly due to the addition of carbon atoms within the cluster.[43, 44] Carboranes are highly tunable, boasting multiple B–H vertices which are amenable to functionalization with a wide array of substituents through well-established methodology.[45-52] Due to the unique electronic character of *ortho*-carborane, substituents attached to boron at the vertices most distal to the carbon atoms experience a strong electronic shielding effect which results in a low chemical shift (methyl C–*H* ≈0.2 ppm) in the ^{1}H NMR spectrum (Figure 1B).[52-54] The hydrophobic nature of carboranes allows them to bind into hydrophobic spaces within proteins and cell membranes, adding potential for their use as affinity labels.[55-58] Additionally, the B–H vibration resonates at ~2350-2600 cm^{-1}, a silent region in Raman spectra of biological milieu, and unique amongst other commonly used Raman tags, such as alkynes and nitriles, which vibrate at ~2000-2300 cm^{-1} (Figure 1B).[59] Herein, we present a new class of functional RAFT agents containing an *ortho*-carborane scaffold. We demonstrate their ability to serve as tunable Raman active molecular probes (Figure 1B), spectroscopic handles for determination of molecular weight *via* ^{1}H NMR spectroscopy, and as affinity labels through β–cyclodextrin binding as judged by isothermal titration calorimetry (ITC) studies.

Results and Discussion

Synthesis of RAFT Agents, Polymerization, and their use as 1H NMR Spectroscopy Handles

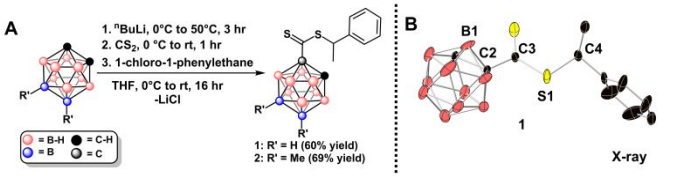

Figure 2. (A) Synthetic scheme for the preparation of carborane RAFT agents **1** and **2**. (B) Solid-state crystal structure of **1**, hydrogen atoms omitted for clarity.

We developed a facile and scalable synthetic method towards carborane-functionalized RAFT agents (Figure 2A). Treatment of a lithiated *o*-carborane slurry in tetrahydrofuran (THF) with carbon disulfide (CS_2) at 0 °C resulted in the formation of a dark red mixture indicating the formation of a sulfide anion which was trapped upon addition of 1-chloro-1-phenylethane to form **1** (Figure 2A). Following column chromatography and crystallization from a saturated solution of CH_2Cl_2 layered with pentane, **1** was isolated as an orange crystalline solid in 60% yield. Single crystals of **1** were grown and subjected to X-ray crystallographic analysis confirming the structural identity of this compound (Figure 2B). We employed **1** in our preliminary polymerization attempts using styrene as the model substrate due to the monomer similarity with the R-group of **1** (Figure 3A).[26]

Figure 3. (A) Thermal polymerization of styrene utilizing either **1** (produces polymer **1-PS**) or **2** (produces polymer **2-PS**) as the RAFT agent. (B) Kinetic analysis for **1-PS** polymerization exhibits first-order kinetics. (C) Evolution of M_n as a function of monomer conversion for **1-PS** polymerization. (D) Table comparing molecular weight determined by ^{1}H NMR spectroscopy and GPC of polymerizations using **1** as the RAFT agent to produce **1-PS** or **2** to produce **2-PS**. Polymerization performed in bulk styrene solution. (E) GPC curves of **2-PS** depicting experiments performed with different equivalents of monomer to CTA (red and black traces) as well as a control in which no CTA is added (blue trace).

Polymerization was carried out in bulk styrene solution and stopped after 4 hours.

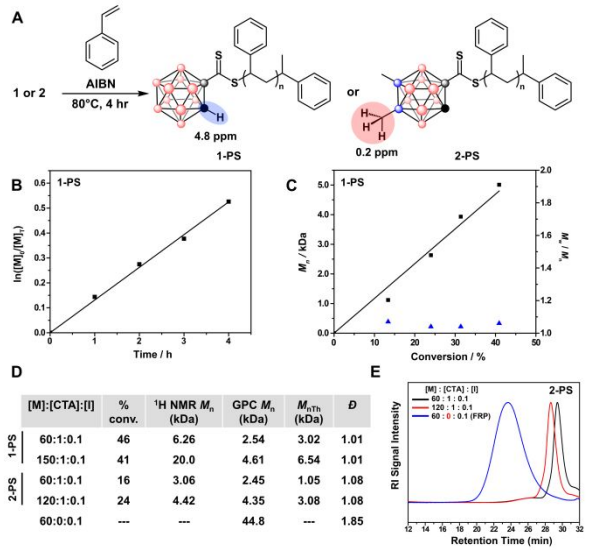

	[M]:[CTA]:[I]	% conv.	^{1}H NMR M_n (kDa)	GPC M_n (kDa)	M_{nTh} (kDa)	$Đ$
1-PS	60:1:0.1	46	6.26	2.54	3.02	1.01
	150:1:0.1	41	20.0	4.61	6.54	1.01
2-PS	60:1:0.1	16	3.06	2.45	1.05	1.08
	120:1:0.1	24	4.42	4.35	3.08	1.08
	60:0:0.1	---	---	44.8	---	1.85

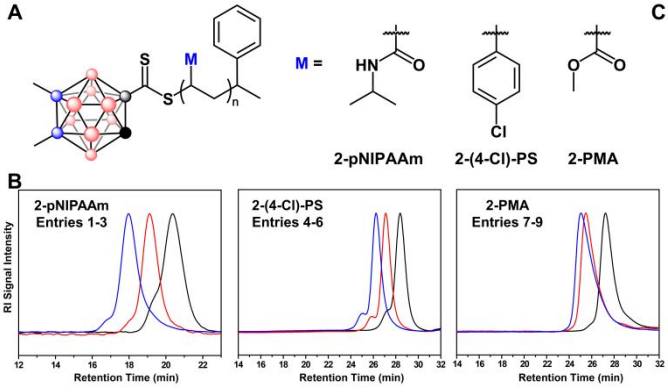

C

	Entry	[M]:[CTA]:[I]	Solvent[a]	% conv	^{1}H NMR M_n (kDa)	GPC M_n (kDa)	M_{nTh} (kDa)[b]	$Đ$
2-pNIPAAm	1	30:1:0.3	PhMe	96	5.84	5.92	3.60	1.10
	2	120:1:0.3	PhMe	93	12.5	11.5	12.9	1.06
	3	180:1:0.3	PhMe	98	20.6	21.3	20.4	1.09
2-(4-Cl)-PS	4	60:1:0.3	Bulk	81	10.7	9.97	7.07	1.08
	5	120:1:0.3	Bulk	56	19.9	18.4	9.67	1.07
	6	180:1:0.3	Bulk	47	27.9	26.6	12.1	1.08
2-PMA	7	60:1:0.3	Bulk	91	11.9	11.4	5.02	1.05
	8	180:1:0.3	Bulk	76	26.7	26.0	12.4	1.03
	9	240:1:0.3	Bulk	74	33.3	29.5	15.5	1.07
2-PS	10	60:1:0.3	EtOAc	33	3.34	3.05	2.18	1.12
	11	60:1:0.3	C_6H_6	43	3.52	3.49	2.83	1.19
	12	60:1:0.3	PhMe	46	4.45	3.52	3.04	1.21
2-PMA	13	60:1:0.3	EtOAc	82	4.95	6.35	4.53	1.13
	14	60:1:0.3	PhMe	82	6.25	5.60	4.53	1.20

Figure 4. (A) Polymerization of methyl acrylate, 4-chlorostyrene, and *N*-isopropylacrylamide. (B) GPC traces for **2-pNIPAAm**, **2-(4-Cl)-PS**, and **2-PMA** at different monomer to CTA ratios. (C) Table depicting results from polymerization experiments performed in bulk reaction conditions and in solvent. [a]Polymerizations were performed in 2 M solvent conditions. [b]Theoretical M_n values were calculated *via* ^{1}H NMR using tetralin as an internal standard.

Polymerization of styrene using 2,2'-azobisisobutyronitrile (AIBN) as the thermal initiator and **1** resulted in nearly monodisperse ($Đ$ = 1.07-1.15) polystyrene (**1-PS**), as determined by gel permeation chromatography (GPC), the length of which was controlled by varying the loading of **1** (Figure 3A, see Figure S11 for GPC traces). Polymerization using **1** exhibits first-order kinetics and a linear evolution of number average molecular weight (M_n) versus conversion, highlighting the controlled nature of the polymerization and demonstrating the utility of carborane-based CTAs in RAFT processes (Figure 3B and 3C). Control experiments in the absence of **1** resulted in highly disperse ($Đ$ = 3.00) polymers indicating loss of control over the polymerization process as expected (See Figure S11). The cage C–H proton of **1** exhibits a diagnostic chemical shift (~4.8 ppm, Figure 3A) which does not overlap with any polystyrene ^{1}H NMR resonances. To investigate the potential usefulness of carboranes to act as spectroscopic probes to accurately determine M_n, we used this highly diagnostic resonance to determine the number average molecular weight (M_n) *via* end-group analysis using ^{1}H NMR spectroscopy. Integration of the carborane C–H proton with the aryl protons of polystyrene resulted in M_n readings which deviated drastically with the M_n values determined by GPC with a multi-angle light scattering (MALS) detector (Figure 3D, see SI for dn/dc values). It is possible to lose the carborane due to its location at the Z group, which would also increase the apparent molecular weight by NMR. However we were unable to find appropriate synthetic conditions to place the carborane at the R group (data not shown). But more likely this deviation is due to the inherent broadness of the carborane cage C–H proton resonance which leads to a higher inaccuracy in M_n determination as the polymer length increases, as is typical for most end groups used for end-group analysis (Figure 3D, **1-PS**; Figure S12). Additionally, the resonance at 4.8 ppm is not located in a generally silent region in most polymer samples, which would eliminate its use as a spectroscopic handle for other types of polymers.

To bypass these complications, we synthesized a carborane derivative bearing methyl groups on the B(9) and B(12) vertices (opposite to those of the carbon atoms) to take advantage of the electronic shielding effect of substituents attached on the B(9) and B(12) vertices, which results in upfield chemical shifts of exohedral methyl proton resonances in ^{1}H NMR spectra and sharper signals.[52, 53, 60] Synthesis of **2** was carried out in a similar manner to that of **1** (Figure 2A). Compound **2** was isolated as a dark orange oil in 69% yield after purification *via* column chromatography and removal of the benzyl chloride precursor by heating under reduced pressure (100 mTorr, 95 °C; Figure 2A; See SI for detailed synthetic procedures). Indeed, the proton signals of the B(9) and B(12) methyl substituents resonate in a characteristic region of the ^{1}H NMR spectrum (~0.2 ppm, See SI). This provides a unique spectroscopic handle as the protons are sufficiently separated from resonances, which may overlap and make for inaccurate M_n determination *via* end-group analysis.

Polymerization of a bulk solution of styrene in the presence of **2** and AIBN produced well-defined ($Đ$ = 1.05–1.06, Figure 3D and 3E) polystyrene (**2-PS**) bearing **2** on the chain end as

determined by ^{1}H NMR after polymer purification *via* precipitation from a cold (0 °C) methanol solution (See SI for characterization of all polymers). To test the accuracy of this method, we made polystyrene using different equivalents of **2** (2.45 and 4.35 kDa, Figure 3D and 3E), determined their M_n values *via* end-group analysis using ^{1}H NMR spectroscopy, and compared the results with those of molecular weight readings measured *via* GPC. In all instances, the M_n values measured with GPC matched closely with the molecular weight determined by ^{1}H NMR spectroscopy (Figure 3D, 3E, see Figures S14, S16, S19, and S22 for example of calculations).

with maintenance of low molecular weight dispersity has been observed in previous reports detailing the RAFT polymerization of acrylamides.[61, 62] However, we find that polymerization in solvent (2M) leads to better agreement between both theoretical and observed M_n values for **2-PMA** (Figure 4, entries 10-14). Control is also maintained over the course of polymerization in solvent in the kinetic plots (Figure S34 and S35). This demonstrates that for these monomers the polymerization should be conducted in solution rather than the bulk phase.

The dithioester carborane end-group allows for a high

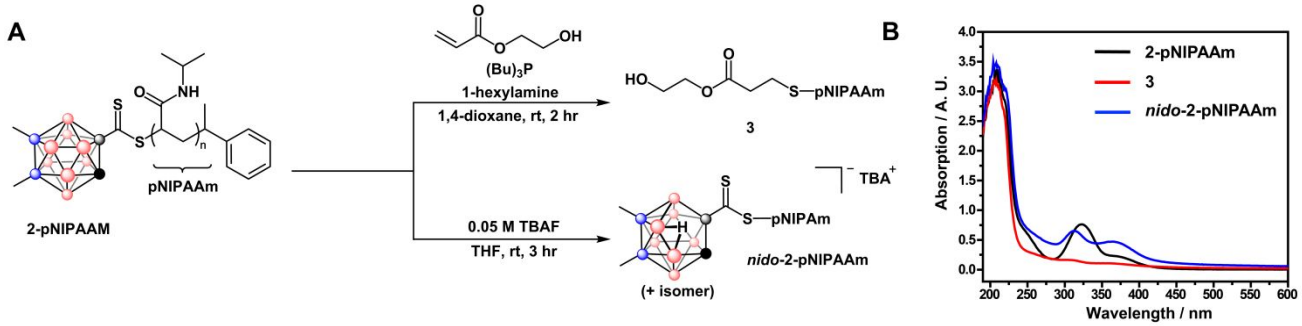

Figure 5. (A) Modification of carborane dithioester end-group of **pNIPAAm**. The end-group can either be removed *via* aminolysis and end-capping or the formation of *nido*-carborane can be achieved via deboronation of carborane using a 0.05 M solution of TBAF in THF. (B) The end-group modification can be followed by UV-Vis spectroscopy. The disappearance of the absorption band at 319 nm indicates the loss of the dithioester. Formation of an absorption band at 375 nm along with a shift in the absorption of the dithioester indicates deboronation of carborane.

We next sought to determine the applicability of **2** with a range of monomers. Matching the "R" and "Z" groups of the RAFT agent to the monomer is vital for controlled RAFT polymerization. As this is the first example of a carborane RAFT agent, we sought to match the R-group with the appropriate monomer classes. We tested *N*-isopropyl acrylamide, methyl acrylate, and 4-chlorostyrene monomers since the reactivity of the benzyl R-group on **2** matches with those monomers.[26] Polymerization of 4-chlorostyrene and *N*-isopropyl acrylamide under thermal polymerization conditions in the presence of 2 and AIBN produced polymers with narrow molecular weight distributions, but with high molecular weight shoulders in the GPC spectra, indicating some polymer coupling (**2-pNIPAAm** and **2-(4-Cl)-PS**, Figure 4A and 4B). Polymerization of methyl acrylate produced monodisperse polymers containing **2** on the polymer chain ends (**2-PMA**, Figure 4A-C and S25). The M_n determined by ^{1}H NMR spectroscopy matches closely with the M_n determined by GPC for a range of polymer sizes (Figure 4B and 4C). Impressively, the methyl C–H protons on carborane are readily visible on the ^{1}H NMR spectrum and are competent spectroscopic handles to accurately determine M_n even at polymer molecular weights up to 30 kDa (Figure 4C, entry 9, and Figure S21). It should be noted that we observe a significant disagreement between the theoretical and observed polymer M_n values for **2-(4-Cl)-PS** and **2-PMA** when polymerized in bulk reaction conditions (Figure 4C, entries 4-9), yet the dispersities remain narrow. This is also apparent in bulk polymer kinetic experiments, which indicate a loss of control over the course of the polymerization (Figure S32). The disagreement between theoretical and observed M_n values

degree of end-group functionality and tunability and can be easily removed or modified after polymerization.[32, 63, 64] We prepared **pNIPAAm** derivatives in which the carborane end-group was removed or deboronated (*vide infra*) to serve as controls for binding studies and to also investigate the properties invoked by having a *nido*-carborane terminated polymer. The carborane end-group of **2-pNIPAAm** was removed *via* aminolysis, thereby leaving an exposed thiol at the polymer end.[63] Despite our use of tributylphosphine to eliminate disulfide formation over the course of the deprotection reaction, we observed polymer coupling by GPC analysis (Figure S36).[65] In order to avoid disulfide formation, we introduced 2-hydroxyethylacrylate which undergoes Michael addition with the exposed thiol thereby attaching onto the end of the polymer and preventing polymer coupling (Figure 5A).[66] The deprotection reaction was monitored *via* UV-Vis spectroscopy by the disappearance of the dithioester absorption band at ~319 nm (Figure 5B). Complete removal of the carborane end-group could also be visualized by ^{1}H NMR spectroscopy after polymer purification by the disappearance of the carborane methyl proton signals at 0.2 ppm.

Deboronation is the partial degradation of the carborane cage where one of the cage boron atoms is stripped away through the use of a strong base. This leads to the formation of an anionic *nido*-carborane species $[7,8\text{-}C_2B_9H_{12}]^-$.[67] Having the monoanionic *nido*-carborane at the polymer end lends potential to interesting self-assembly properties as the polymer is rendered amphiphilic. Additionally, *nido*-carborane is used frequently to bind metal ions thereby forming metallacarboranes.[68, 69] One can envisage the binding of metal

ions in this system to synthesize block co-polymers and other higher order macromolecular architectures.[70] Preparation of *nido*-carborane terminated pNIPAAm (***nido*-2-pNIPAAm**) was carried out by stirring **2-pNIPAAm** in a solution of 0.05 M tetrabutylammonium fluoride (TBAF) in THF (Figure 5A).[71] We were unable to follow deboronation by ^{11}B NMR or ^{13}C NMR due to the large size of the polymer relative to the carborane end-group. However, over the course of the reaction we noticed a diagnostic resonance corresponding to the formed hydride in the ^{1}H NMR spectrum at -2.1 ppm (Figure S38). We also followed deboronation by the appearance of a new UV band at ~375 nm as well as a shift of the dithioester absorption band (Figure 5B).

Binding Studies with Polymers Terminated with Functional

We measured binding of **2-pNIPAAm** to β-cyclodextrin *via* isothermal titration calorimetry (ITC) in MilliQ water. A solution of a known concentration of β-cyclodextrin was titrated into a solution of **2-pNIPAAm**. Based on the titration curve, we calculated a K_a of 9.37 x 10^4 M^{-1} which agrees with previous literature reports of free carborane binding in the hydrophobic pocket of β-cyclodextrin (Figure 6A). An N=0.5 value was also calculated, which is indicative of a 2:1 binding of carborane to β-cyclodextrin. While the binding of two carborane groups into β-cyclodextrin has not been reported, it is possible that the substituents on the carborane end-group of **2-pNIPAAm** block full incorporation of one carborane unit into β-cyclodextrin thereby allowing room for a second unit to partially bind. We were unable to perform the reverse titration due a lack of solubility of **2-pNIPAAm** in water at high concentrations.

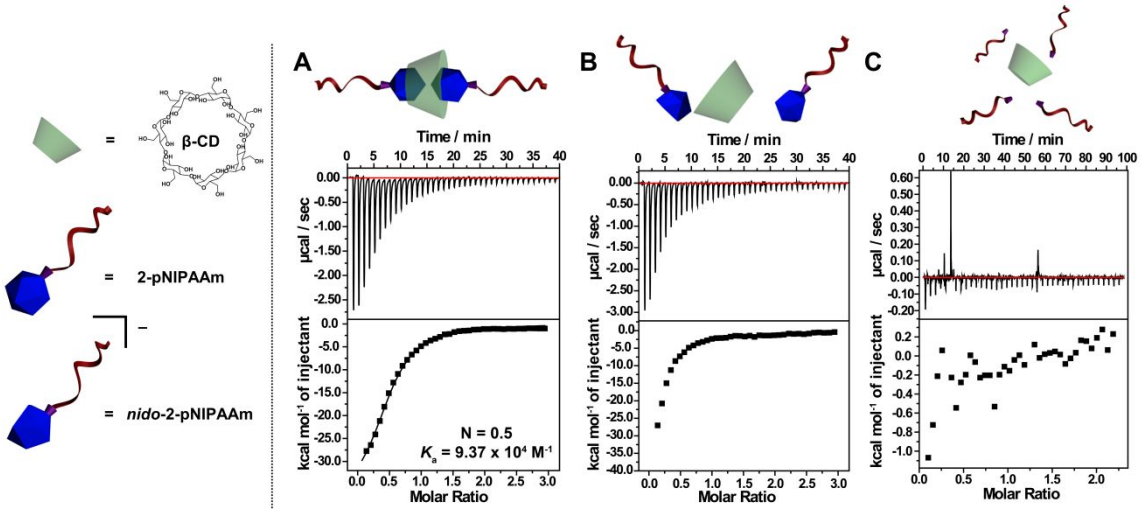

Figure 6. (A) ITC curve of a 0.1 mM solution of **2-pNIPAAm** titrated into a 1.06 mM β-cyclodextrin solution shows 2:1 binding (N=0.5). (B) ITC curve of ***nido*-2-pNIPAAm** shows only minimal binding (N=0.06) which can be attributed to small amounts of **2-pNIPAAm** still present in solution. The inability of ***nido*-2-pNIPAAm** to bind to β-cyclodextrin can possibly be attributed to the bulkiness of the TBA^+ counterion present on the polymer chain end. (C) ITC curve of **3** and β-cyclodextrin shows no observable binding.

Carborane Handles

Affinity tags such as biotin are frequently exploited within the chemical biology community in purification and detection strategies such as in tandem orthogonal proteolysis-activity-based protein profiling (TOP-ABPP) and enzyme-linked immunosorbent assay (ELISA).[72, 73] To probe the ability of carborane appended onto a polymer chain to act as an affinity tag, we investigated the binding of **2-pNIPAAm**, ***nido*-2-pNIPAAm**, and **3** to β–cyclodextrin, a cyclic molecule composed of seven α-D-glucopyranoside units. The hydrophobic inner cavity of β–cyclodextrin is well-suited for the incorporation of hydrophobic guests thereby forming host-guest inclusion complexes through non-covalent bonding interactions. Carboranes are known to form 1:1 and 2:1 inclusion complexes with β-cyclodextrin exhibiting association constants (K_a) as strong as ≈ 10^6 M^{-1}.[74-78] Previous studies have shown this interaction as a means to solubilize carborane scaffolds in aqueous solutions and for the immobilization of biomolecules on surfaces.[79, 80]

We observed a negligible amount of binding (N=0.06) when we carried out similar ITC studies with ***nido*-2-pNIPAAm** (Figure 6B). While the binding of *nido*-carboranes to β-cyclodextrin has not been studied, *nido*-carborane drug derivatives were shown to bind in the hydrophobic sub-pockets of the proteins carbonic anhydrase (CA) and cyclooxygenase-2 (COX-2).[81, 82] It is likely that in this instance, the bulkiness of the TBA^+ counterion does not allow for binding of ***nido*-2-pNIPAAm** in the hydrophobic β-cyclodextrin pocket. Likewise, compound **3** does not exhibit any detectable binding, highlighting that only polymer samples terminated with carborane end-groups can undergo self-assembly processes thereby emphasizing their potential application in affinity labeling (Figure 6C).

Carborane CTA for use in Raman Spectroscopy and Self-Assembly Processes

Raman spectroscopy, especially stimulated Raman spectroscopy (SRS), is emerging as a powerful technique for use in bioimaging.[83] Although fluorescence techniques still remain ubiquitous, there are many inherent limitations which include photobleaching of small molecule dyes, which shortens their lifetimes, and the need to use external chemical or photophysical stimuli which could damage biological samples.[83] Raman spectroscopy bypasses these limitations by relying on the inherent molecular vibrations in samples. Label-free Raman spectroscopy has been utilized in the analysis of biological samples, primarily investigating bond vibrational signals in the fingerprint (500–1700 cm^{-1}) region as well as higher regions (2800–3200 cm^{-1}).[83] However, there is a need to develop Raman active labels as a way to overcome limitations with label-free analysis which include difficulty in differentiating signals within biological media, weak signal-to-noise ratios, and the inability to track molecules within samples. Because the B–H vibrational signal (~2350–2600 cm^{-1}) of carborane compounds appear in silent regions within the Raman spectra of biological samples (~1740–2800 cm^{-1}), they are ideally suited to serve as bioorthogonal molecular probes for Raman applications.[59, 83]

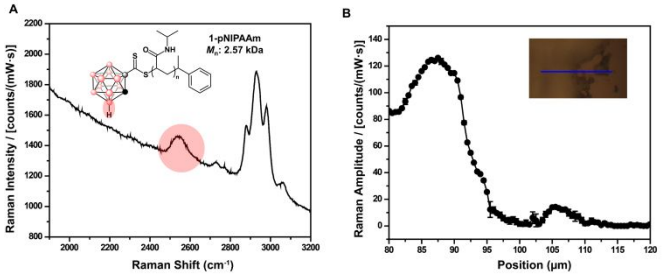

Figure 7. (A) Representative Raman spectrum of **1-pNIPAAm** thin film indicating B-H Raman signal at 2549 cm^{-1}. (B) Film-edge Raman scan of a **1-pNIPAAm** thin film showing Raman activity only in areas where the polymer is present. Inset: optical image of the thin film analyzed, the blue line denotes the region scanned.

We first analyzed the polymers *via* infrared spectroscopy and found that despite the carborane only accounting for 144 Da of polymers ranging 2,000 to 6,000 Da, we still observed the B–H vibrational signal (Figures S39 and S40). To demonstrate the potential utility of carborane terminated polymers to act as probes for Raman imaging, a thin film of 1-pNIPAAm on a glass substrate was scanned using spontaneous Raman scattering. The B–H vibration occurs at a unique frequency (2549 cm^{-1}) that is isolated from the C–H stretch region in a Raman-silent of biological samples (Figure 7A). We also drop-cast a thin-film of **1-pNIPAAm** on a quartz substrate and performed a Raman scan at the edge of the film. A significant Raman amplitude at 2549 cm^{-1} is observed only in areas where the thin film is present, the amplitude quickly drops off when scanning over areas where the **1-pNIPAAm** film is absent (Figure 7B). The intensity of the B–H Raman vibration is also worthy to note in this application, with an estimated cross section per bond that is 3 times that of a typical C-H stretching mode cross section (SI). This experiment therefore demonstrates the potential utility of the B–H vibrational stretches inherent to carboranes for Raman imaging in polymer materials made via controlled polymerization.

Conclusions

In summary, we present the utilization of tunable carborane functionalized RAFT agents. We investigated their ability to control polymerization processes of multiple monomer classes, and to serve as universal ^{1}H NMR spectroscopic handles, affinity labels, and Raman active molecular probes. We were able to accurately determine polymer molecular weight *via* end-group analysis using ^{1}H NMR spectroscopy. ITC studies of carborane terminated pNIPAAm samples showed a 2:1 (carborane: β-cyclodextrin) binding with a K_a value of 9.37 x 10^4 M^{-1}. Similar studies using *nido*-carborane terminated pNIPAAm and pNIPAAm samples without carborane end-groups showed no binding to β-cyclodextrin. Additionally, the B–H bonds on carborane are able to act as a Raman active spectroscopic probes with a vibrational signal (2350-2600 cm^{-1}), a Raman silent region of biological samples. This new class of RAFT agents adds to the expanding chemical toolbox available to biologists, chemists, and materials scientists while providing a new avenue of study at the intersection of main-group chemistry and polymer materials.[84-89]

Conflicts of interest

There are no conflicts to declare.

Acknowledgements

A.M.S. thanks UCLA Department of Chemistry and Biochemistry for start-up funds and 3M for a Non-Tenured Faculty Award. M.S.M. thanks the NSF for the Bridge-to-Doctorate (HRD-1400789) and the Predoctoral (GRFP) (DGE-0707424) Fellowships and UCLA for the Christopher S. Foote Fellowship. O.M.E. thanks the Raymond and Dorothy Wilson Fellowship. H.D.M. thanks the NSF (CHE-1507735) for funding. C.T.G. and R.R.F. thank the NSF (CHE-1552849) for funding. P. C. thanks the Gold Family Foundation and the SPE Foundation for funding. The authors would like to thank the UCLA-DOE and Biochemistry Instrumentation Facility for providing access to the ITC instrument and for helpful discussions relating to the data acquisition.

Notes and references

1. H. Gao and K. Matyjaszewski, *Prog. Polym. Sci.*, 2009, **34**, 317-350.
2. M. Bathfield, F. D'Agosto, R. Spitz, M.-T. Charreyre and T. Delair, *J. Am. Chem. Soc.*, 2006, **128**, 2546-2547.
3. B. R. Elling and Y. Xia, *ACS Macro Lett.,* 2018, **7**, 656-661.

4. C. A. Figg, A. N. Bartley, T. Kubo, B. S. Tucker, R. K. Castellano and B. S. Sumerlin, *Polym. Chem.*, 2017, **8**, 2457-2461.
5. M. Päch, D. Zehm, M. Lange, I. Dambowsky, J. Weiss and A. Laschewsky, *J. Am. Chem. Soc.*, 2010, **132**, 8757-8765.
6. D. Vinciguerra, J. Tran and J. Nicolas, *Chem. Commun.*, 2018, **54**, 228-240.
7. Y. Bao, E. Guégain, V. Nicolas and J. Nicolas, *Chem. Commun.*, 2017, **53**, 4489-4492.
8. S. Liu, Y. Cheng, H. Zhang, Z. Qiu, R. T. Kwok, J. W. Lam and B. Z. Tang, *Angew. Chem. Int. Ed.*, 2018, **57**, 6274-6278.
9. B. S. Tucker, J. D. Stewart, J. I. Aguirre, L. S. Holliday, C. A. Figg, J. G. Messer and B. S. Sumerlin, *Biomacromolecules*, 2015, **16**, 2374-2381.
10. C. P. Ryan, M. E. Smith, F. F. Schumacher, D. Grohmann, D. Papaioannou, G. Waksman, F. Werner, J. R. Baker and S. Caddick, *Chem. Commun.*, 2011, **47**, 5452-5454.
11. V. Coessens, T. Pintauer and K. Matyjaszewski, *Prog. Polym. Sci.*, 2001, **26**, 337-377.
12. Y. Bao, E. Guégain, J. Mougin and J. Nicolas, *Polym. Chem.*, 2018.
13. K. Matyjaszewski and N. V. Tsarevsky, *Nat. Chem.*, 2009, **1**, 276.
14. B. Le Droumaguet and J. Nicolas, *Polym. Chem.*, 2010, **1**, 563-598.
15. F. Lecolley, L. Tao, G. Mantovani, I. Durkin, S. Lautru and D. M. Haddleton, *Chem. Commun.*, 2004, 2026-2027.
16. W. Agut, D. Taton and S. Lecommandoux, *Macromolecules*, 2007, **40**, 5653-5661.
17. K. Matyjaszewski, *Macromolecules*, 2012, **45**, 4015-4039.
18. C.-Y. Hong and C.-Y. Pan, *Macromolecules*, 2006, **39**, 3517-3524.
19. S. Martens, F. Driessen, S. Wallyn, O. u. Türünç, F. E. Du Prez and P. Espeel, *ACS Macro Lett.*, 2016, **5**, 942-945.
20. J. Chiefari, Y. Chong, F. Ercole, J. Krstina, J. Jeffery, T. P. Le, R. T. Mayadunne, G. F. Meijs, C. L. Moad and G. Moad, *Macromolecules*, 1998, **31**, 5559-5562.
21. C. Boyer, V. Bulmus, T. P. Davis, V. Ladmiral, J. Liu and S. Perrier, *Chem. Rev.*, 2009, **109**, 5402-5436.
22. G. Moad, E. Rizzardo and S. H. Thang, *Aust. J. Chem.*, 2012, **65**, 985-1076.
23. G. Moad, E. Rizzardo and S. H. Thang, *Chem. Asian J.*, 2013, **8**, 1634-1644.
24. J. Bernard, X. Hao, T. P. Davis, C. Barner-Kowollik and M. H. Stenzel, *Biomacromolecules*, 2006, **7**, 232-238.
25. S. b. Perrier, *Macromolecules*, 2017, **50**, 7433-7447.
26. G. Moad, E. Rizzardo and S. H. Thang, *Acc. Chem. Res.*, 2008, **41**, 1133-1142.
27. D. J. Keddie, G. Moad, E. Rizzardo and S. H. Thang, *Macromolecules*, 2012, **45**, 5321-5342.
28. M. J. Monteiro, *J. Polym. Sci. A: Polym. Chem.*, 2005, **43**, 3189-3204.
29. J. Skey and R. K. O'Reilly, *Chem. Commun.*, 2008, 4183-4185.
30. J. Chiefari, R. T. Mayadunne, C. L. Moad, G. Moad, E. Rizzardo, A. Postma, M. A. Skidmore and S. H. Thang, *Macromolecules*, 2003, **36**, 2273-2283.
31. D. Estupinan, T. Gegenhuber, J. P. Blinco, C. Barner-Kowollik and L. Barner, *ACS Macro Lett.*, 2017, **6**, 229-234.
32. G. Moad, E. Rizzardo and S. H. Thang, *Polym. Int.*, 2011, **60**, 9-25.
33. C. Boyer, V. Bulmus, P. Priyanto, W. Y. Teoh, R. Amal and T. P. Davis, *J. Mater. Chem.*, 2009, **19**, 111-123.
34. V. Vázquez-Dorbatt, Z. P. Tolstyka and H. D. Maynard, *Macromolecules*, 2009, **42**, 7650-7656.
35. S. J. Paluck and H. D. Maynard, *Polym. Chem.*, 2017, **8**, 4548-4556.
36. J. Xu, C. Boyer, V. Bulmus and T. P. Davis, *J. Polym. Sci. A: Polym. Chem.*, 2009, **47**, 4302-4313.
37. M. Li, P. De, S. R. Gondi and B. S. Sumerlin, *Macromol. Rapid Commun.*, 2008, **29**, 1172-1176.
38. M. P. Robin, M. W. Jones, D. M. Haddleton and R. K. O'Reilly, *ACS Macro Lett.*, 2011, **1**, 222-226.
39. M. M. Lorenzo, C. G. Decker, M. U. Kahveci, S. J. Paluck and H. D. Maynard, *Macromolecules*, 2015, **49**, 30-37.
40. L. McDowall, G. Chen and M. H. Stenzel, *Macromol. Rapid Commun.*, 2008, **29**, 1666-1671.
41. C. Boyer, V. Bulmus, J. Liu, T. P. Davis, M. H. Stenzel and C. Barner-Kowollik, *J. Am. Chem. Soc.*, 2007, **129**, 7145-7154.
42. J. T. Lai, D. Filla and R. Shea, *Macromolecules*, 2002, **35**, 6754-6756.
43. R. N. Grimes, *Carboranes*, Academic Press, 2016.
44. A. M. Spokoyny, *Pure Appl. Chem.*, 2013, **85**, 903-919.
45. Z. Qiu, *Tetrahedron Lett.*, 2015, **56**, 963-971.
46. R. M. Dziedzic, J. L. Martin, J. C. Axtell, L. M. Saleh, T.-C. Ong, Y.-F. Yang, M. S. Messina, A. L. Rheingold, K. N. Houk and A. M. Spokoyny, *J. Am. Chem. Soc.*, 2017, **139**, 7729-7732.
47. R. M. Dziedzic, L. M. Saleh, J. C. Axtell, J. L. Martin, S. L. Stevens, A. T. Royappa, A. L. Rheingold and A. M. Spokoyny, *J. Am. Chem. Soc.*, 2016, **138**, 9081-9084.
48. A. M. Spokoyny, C. W. Machan, D. J. Clingerman, M. S. Rosen, M. J. Wiester, R. D. Kennedy, C. L. Stern, A. A. Sarjeant and C. A. Mirkin, *Nat. Chem.*, 2011, **3**, 590-596.
49. R. Cheng, Z. Qiu and Z. Xie, *Nat. Commun.*, 2017, **8**, 14827.
50. Z. Qiu, Y. Quan and Z. Xie, *J. Am. Chem. Soc.*, 2013, **135**, 12192-12195.
51. W.-B. Yu, P.-F. Cui, W.-X. Gao and G.-X. Jin, *Coord. Chem. Rev.*, 2017, **350**, 300-319.
52. Z. Zheng, W. Jiang, A. A. Zinn, C. B. Knobler and M. F. Hawthorne, *Inorg. Chem.*, 1995, **34**, 2095-2100.
53. F. Teixidor, G. Barberà, A. Vaca, R. Kivekäs, R. Sillanpää, J. Oliva and C. Viñas, *J. Am. Chem. Soc.*, 2005, **127**, 10158-10159.
54. A. M. Spokoyny, C. D. Lewis, G. Teverovskiy and S. L. Buchwald, *Organometallics*, 2012, **31**, 8478-8481.
55. M. P. Grzelczak, S. P. Danks, R. C. Klipp, D. Belic, A. Zaulet, C. Kunstmann-Olsen, D. F. Bradley, T. Tsukuda, C. Viñas and F. Teixidor, *ACS Nano*, 2017, **11**, 12492-12499.
56. A. F. Armstrong and J. F. Valliant, *Dalton Trans.*, 2007, 4240-4251.
57. D. Gabel, *Pure Appl. Chem.*, 2015, **87**, 173-179.
58. J. F. Valliant, K. J. Guenther, A. S. King, P. Morel, P. Schaffer, O. O. Sogbein and K. A. Stephenson, *Coord. Chem. Rev.*, 2002, **232**, 173-230.
59. D. C. Kennedy, D. R. Duguay, L.-L. Tay, D. S. Richeson and J. P. Pezacki, *Chem. Commun.*, 2009, 6750-6752.
60. A. Siedle, G. Bodner, A. Garber, D. Beer and L. Todd, *Inorg. Chem.*, 1974, **13**, 2321-2324.
61. M. S. Donovan, A. B. Lowe, B. S. Sumerlin and C. L. McCormick, *Macromolecules*, 2002, **35**, 4123-4132.
62. D. B. Thomas, A. J. Convertine, L. J. Myrick, C. W. Scales, A.

E. Smith, A. B. Lowe, Y. A. Vasilieva, N. Ayres and C. L. McCormick, *Macromolecules*, 2004, **37**, 8941-8950.
63. H. Willcock and R. K. O'Reilly, *Polym. Chem.*, 2010, **1**, 149-157.
64. H. Golf, R. O'Shea, C. Braybrook, O. E. Hutt, D. W. Lupton and J. Hooper, *Chem. Sci.*, 2018, **9**, 7370-7375.
65. M. Li, P. De, S. R. Gondi and B. S. Sumerlin, *J. Polym. Sci. A: Polym. Chem.*, 2008, **46**, 5093-5100.
66. J. M. Spruell, B. A. Levy, A. Sutherland, W. R. Dichtel, J. Y. Cheng, J. F. Stoddart and A. Nelson, *J. Polym. Sci. A: Polym. Chem.*, 2009, **47**, 346-356.
67. M. F. Hawthorne, D. C. Young, P. M. Garrett, D. A. Owen, S. G. Schwerin, F. N. Tebbe and P. A. Wegner, *J. Am. Chem. Soc.*, 1968, **90**, 862-868.
68. M. F. Hawthorne, D. C. Young and P. A. Wegner, *J. Am. Chem. Soc.*, 1965, **87**, 1818-1819.
69. R. N. Grimes, *Coord. Chem. Rev.*, 2000, **200**, 773-811.
70. A. V. Safronov, Y. V. Sevryugina, K. R. Pichaandi, S. S. Jalisatgi and M. F. Hawthorne, *Dalton Trans.*, 2014, **43**, 4969-4977.
71. M. Fox, W. Gill, P. Herbertson, J. MacBride, K. Wade and H. Colquhoun, *Polyhedron*, 1996, **15**, 565-571.
72. E. Weerapana, A. E. Speers and B. F. Cravatt, *Nat. Protoc.*, 2007, **2**, 1414.
73. C. Kendall, I. Ionescu-Matiu and G. R. Dreesman, *J. Immunomol. Methods*, 1983, **56**, 329-339.
74. K. Ohta, S. Konno and Y. Endo, *Tetrahedron Lett.*, 2008, **49**, 6525-6528.
75. R. Vaitkus and S. Sjöberg, *J. Incl. Phenom. Macrocycl. Chem.*, 2011, **69**, 393-395.
76. K. Sadrerafi, E. E. Moore and M. W. Lee, *J. Incl. Phenom. Macrocycl. Chem.*, 2015, **83**, 159-166.
77. A. Harada and S. Takahashi, *J. Chem. Soc., Chem. Commun.*, 1988, 1352-1353.
78. J. Nekvinda, B. Grüner, D. Gabel, W. Nau and K. Assaf, *Chem. Eur. J.*, 2018, **24**, 12970-12975.
79. H. Xiong, D. Zhou, X. Zheng, Y. Qi, Y. Wang, X. Jing and Y. Huang, *Chem. Commun.*, 2017, **53**, 3422-3425.
80. P. Neirynck, J. Schimer, P. Jonkheijm, L.-G. Milroy, P. Cigler and L. Brunsveld, *J. Mater. Chem. B*, 2015, **3**, 539-545.
81. W. Neumann, S. Xu, M. B. Sárosi, M. S. Scholz, B. C. Crews, K. Ghebreselasie, S. Banerjee, L. J. Marnett and E. Hey-Hawkins, *ChemMedChem*, 2016, **11**, 175-178.
82. J. Brynda, P. Mader, V. Šícha, M. Fábry, K. Poncová, M. Bakardiev, B. Grüner, P. Cígler and P. Řezáčová, *Angew. Chem.*, 2013, **125**, 14005-14008.
83. L. Wei, F. Hu, Z. Chen, Y. Shen, L. Zhang and W. Min, *Acc. Chem. Res.*, 2016, **49**, 1494-1502.
84. T. Dellermann, N. E. Stubbs, D. A. Resendiz-Lara, G. R. Whittell and I. Manners, *Chem. Sci.*, 2018, **9**, 3360-3366.
85. G. M. Adams, A. L. Colebatch, J. T. Skornia, A. I. McKay, H. C. Johnson, G. C. Lloyd− Jones, S. A. Macgregor, N. A. Beattie and A. S. Weller, *J. Am. Chem. Soc.*, 2018, **140**, 1481-1495.
86. S. N. Mendis, T. Zhou and R. S. Klausen, *Macromolecules*, 2018, **51**, 6859-6864.
87. Y. Adachi, Y. Ooyama, Y. Ren, X. Yin, F. Jäkle and J. Ohshita, *Polym. Chem.*, 2018, **9**, 291-299.
88. S. Ye, M. Steube, E. I. Carrera and D. S. Seferos, *Macromolecules*, 2016, **49**, 1704-1711.
89. F. Jäkle and F. Vidal, *Angew. Chem. Int. Ed.,* 2019, DOI: 10.1002/anie.201810611.

Carborane RAFT agents are introduced as tunable multi-purpose tools acting as ^{1}H NMR spectroscopic handles, Raman probes, and recognition units.